Spurious-Mode Suppression in Optoelectronic Oscillators

Olukayode Okusaga
and Eric Adles
and Weimin Zhou
U.S. Army Research Laboratory
Adelphi, Maryland 20783–1197
Email: olukayode.okusaga@us.army.mil

Curtis Menyuk
and Gary Carter
Department of Computer Science
and Electrical Engineering
1000 Hilltop Circle
Baltimore, Maryland 21850

Etgar Levy
and Moshe Horowitz
Technion Institute of Technology
Haifa, Israel

***Abstract*—Optoelectronic oscillators (OEOs) are promising low phase noise radio frequency sources. However, the long fiber loops required for a high Oscillator Q also lead to spurious modes (spurs) spaced too narrowly to be filtered by standard electronic devices. As a solution to this problem, the dual injection-locked OEo (DIL-OEO) has been proposed and studied. Previously, we presented experimental data demonstrating spur suppression in the DIL-OEO. We also developed theoretical models enabling us to optimize the DIL-OEO. In this work, we present data demonstrating 60 dB suppression of the nearest-neighbour spur in a high-Q OEO without increasing the phase noise within 1 kHz of the 10 GHz oscillating mode.**

I. Introduction

An optolectronic oscillator (OEO) is a radio frequency (RF) oscillator that utilizes an optical fiber delay line as a high-Q resonant cavity [1], [2]. The low loss-per-unit-length of standard single-mode optical fiber, allows for OEOs with delay lines as long as 16 km and Q-factors as high as 4×10^6 [3]. Due to the high Q of cavities made from long optical fiber delay lines, OEOs are capable of generating very low phase noise RF signals.

Fig. 1 shows a schematic of the single-loop OEO. The OEO consists of a continuous wave (CW) laser, an electro-optic modulator, an optical fiber delay line, a photodetector, an RF amplifier block, an RF filter, and an RF output coupler. The OEO is an electro-optic ring oscillator. At the optical modulator, the RF signal amplitude modulates the laser output beam. The modulated optical beam travels along the optical fiber delay line which induces a group delay τ in the modulated beam. At the photodetector, the delayed RF signal is recovered. The photodetector output signal is amplified and filtered. A portion of the filtered signal is coupled out of the OEO. The remainder of the filtered signal is fed back into the optical modulator, thereby completing the RF-photonic ring. The laser, modulator, optical fiber, and photodetector form an RF-photonic link that induces much greater delays than are possible with standard RF delay lines. Fig. 2 shows a diagram of the DIL-OEO. The DIL-OEO consists of two coupled OEO loops. A long master loop provides high Q, but has many cavity modes that are typically spaced 10–100 kHz apart. It is not desirable to have more than one mode oscillating at once. The unwanted modes are referred to as spurious modes or

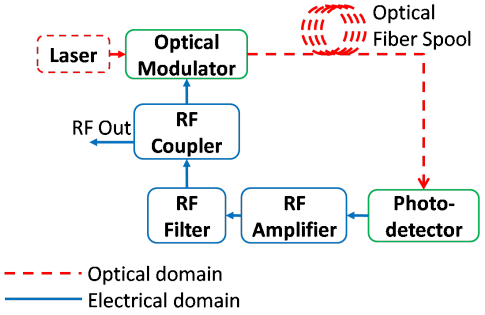

Fig. 1. A schematic diagram of the single-loop OEO.

spurs, and these modes are too closely spaced to be eliminated with an RF filter. A shorter slave loop has lower Q, but has a wider mode spacing. A portion of the master signal is injected into the slave loop and vice versa. As we have shown in previous work, this bi-directional injection is the key to achieving both low phase noise and low spurs [4]. The master-to-slave injection ensures that the DIL-OEO maintains a high Q. The slave-to-master injection ensures spur suppression and helps to maintain a stable phase-lock between both loops. In this work, we present experimental data from our optimized DIL-OEO. We optimized the DIL-OEO by increasing both the length of the slave loop and the coupling between the master and slave loops. We present experimental data that shows the effects of varying the slave loop length and coupling strength on the phase noise and spurs of a DIL-OEO. Our optimized DIL-OEO exhibits the low phase noise of a high-Q single-loop OEO, but with significantly suppressed spurs. Relative to the free-running master loop, we obtained 60 dB spur suppression with no phase noise penalty below 1 kHz and only an 8 dB phase noise penalty at 10 kHz offset frequency.

II. Experimental Setup

A. Master and Slave Loops

The master and slave loops each contain a single CW laser, a lithium niobate modulator, a length of optical fiber, a photodiode, a series of radio-frequency (RF) amplifiers, directional couplers leading to the injection bridge, an RF

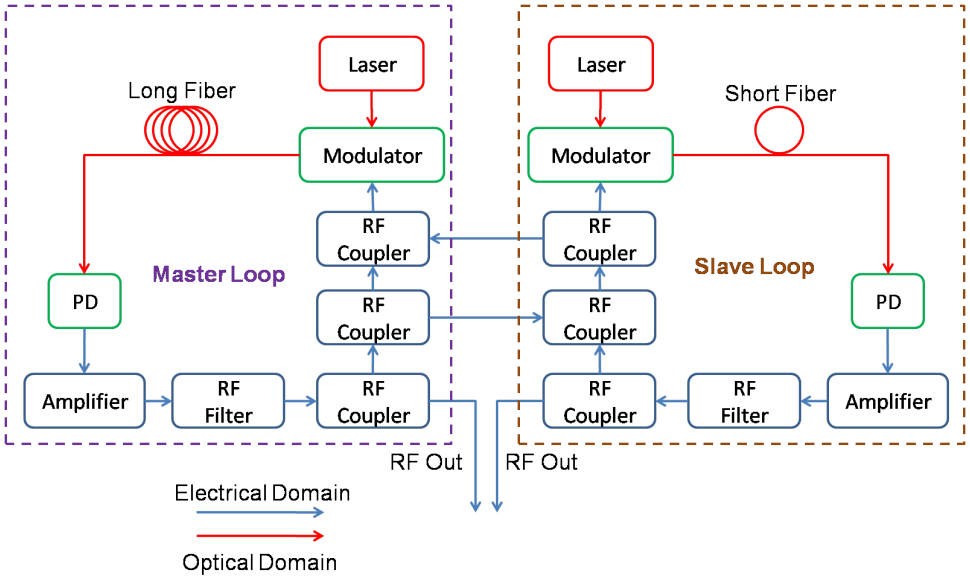

Fig. 2. Schematic diagram of the DIL-OEO.

filter and output couplers to the measurement system. The CW lasers are distributed feedback (DFB) semiconductor diode lasers. We use standard Corning SMF-28 single-mode fiber in all measurements.

For the injection-locking study, we used a 4 km master loop length. We used two different slave loop lengths in this study: 44 m, and 547 m. We chose these slave loop lengths so that the slave loop was either single mode within the bandwidth of the in-loop bandpass filter, or supported no spurious modes closer than 500 kHz to the central RF frequency tone.

The photodetectors that we used were p-i-n photodiodes with RF 3 dB bandwidths of 12 GHz. We used specially designed low-phase-noise RF amplifiers in both loops. The amplifiers have phase noise levels of –155 dBc/Hz at a 1 kHz offset, noise figures of –6.5 dB, small-signal gains of 22 dB, bandwidths of 2 GHz at the 3 dB rolloff frequencies, and saturation output powers of 24 dBm at 10 GHz. The RF bandpass filters had 10 GHz central frequencies with bandwidths of 8 MHz. The RF filters ensured that the DIL-OEOs oscillated close to 10 GHz. The slave loop also included a tunable RF phase shifter. The phase shifter was used to tune the resonant frequency of the slave loop so that it was close enough to one of the resonant modes of the master loop to ensure a phase lock between both loops.

Output couplers in both loops allowed us to measure their oscillating signals independently. The output couplers were placed immediately after the final RF amplifier to ensure that the RF signal was measured at its maximum amplitude in the loop. The output powers were approximately 15 dBm. In all of our measurements, the equilibrium oscillating power at the output couplers of the master and slave loops were within 1 dB of each other. Nearly identical equilibrium powers in both master and slave loops were achieved by using RF amplifiers with similar saturation powers in both loops.

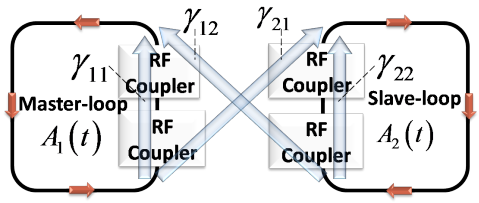

Fig. 3. A schematic diagram of the bi-directional injection bridge. The Γ_{ij} are power coupling ratios.

B. Bi-directional Injection Bridge

The injection bridge was designed to allow us to study both forward and reverse injection independently. Both the master and slave loops contain output and input couplers. The bi-directional bridge consists of two arms. One arm leads from the master loop's output coupler to an isolator, a variable attenuator, and into the slave loop's input coupler. The other arm of the bridge is designed in reverse fashion with an isolator after the slave loop's output coupler, followed by a variable isolator and ending in the input coupler of the master loop. The isolators in each arm provide 1 dB of loss in their forward directions while providing 20 dB loss in their reverse directions. The isolators allow us to ensure that 99% of the master-to-slave injection occurs in the forward injection arm and similarly, 99% of the slave-to-master injection occurs in the reverse injection arm. The variable attenuators allow us to vary the levels of forward and reverse injection independently within a limitted range. Fig. 3 shows a schematic diagram of the bi-directional injection bridge. The Γ_{ij} terms are the power splitting ratios in the bridge, where "1" refers to the master loop and "2" refers to the slave. We used –3dB power dividers as input and output couples in both master and slave loops. Attenuation in the bridge can affect the equilibrium

power levels in both master and slave loops. Changes in the equilibrium power level in either loop may alter both the phase noise and spur levels of the DIL-OEO. We found it best to place the strong injection bridge after the final amplifier in both loops. Gain saturation in the final amplifier ensures that the input signal levels into the bridge at equilibrium remain constant even as forward and reverse injection ratios are varied.

C. Injection-Locking Parameters

The injection-locking parameters studied in this work are the coupling strength and the slave loop's length. By altering these prameters, we were able to vary both the phase noise and spur levels in the DIL-OEO. In previous work, we demonstrated that increasing the injection level from the master loop to the slave loop reduced phase noise, while increasing spur levels in both loops of the DIL-OEO [4]–[6]. Conversely, increasing the injection level from the slave loop to the master loop increased phase noise while decreasing spur levels in both the master and slave loops. In this study, we investigated the effects of varying the master-to-slave and slave-to-master injection levels in unison.

We define the coupling ratio C as the ratio of the power injection from the master to slave to the power in the master loop after the bridge. We found that keeping the master-to-slave and slave-to-master injection level equal produced the best results. Because the oscillating powers in both loops were equal, the coupling ratio is given by

$$C \equiv \frac{\Gamma_{21}}{\Gamma_{11}} \approx \frac{\Gamma_{12}}{\Gamma_{22}}. \tag{1}$$

The coupling levels used in this study were 0 dB, –3 dB, –6 dB, –10 dB, and –20 dB.

We also studied the the effects of varying the slave loop's length. The slave loop acts as a frequency discriminator that filters out spurious modes from the master loop. The longer the slave loop the narrower its effective filter bandwidth becomes. Increasing the slave loop's length should reduce the level of spurs closest to he central oscillating mode. However, increasing the slave loop's length, decreases the mode spacing of the slave. Once the slave becomes multi-mode within the RF filter's bandwidth, the power levels of some spurious modes should increase. In this work, we present experimental data showing the net effect of increasing the slave loop's length on the phase noise and spurs in the DIL-OEO.

III. Experimental Data and Analysis

We used a delay line phase noise measurement system to collect the experimental data presented in this work. As we varied both injection-locking parameters, we measured the phase noise of the output signals from both the master and slave loops. From our phase noise data, we identify effects of the injection-locking parameters on the DIL-OEO phase noise and spur levels.

A. Slave Loop Length

In order to investigate the effect of the slave loop's length on the spurs, we constructed DIL-OEOs using two slave loop lengths: 44 m, and 547 m. The master loop length was fixed at 4 km. The forward and reverse injection ratios were fixed at –18 dB. We then collected phase noise data from both the master and slave loops of each DIL-OEO configuration. Fig. 4 shows the phase noise data from both the master and slave loops for both DIL-OEO configurations. Fig. 4(a) shows that increasing the slave loop's length had no effect on the master loop phase noise. However, increasing the slave loop length reduced the first and second spurs in the master loop by 20 and 8 dB respectively. In fact, all of the master loops spurs were reduced by increasing slave loop length including the master spur closest to the free-running slave loop spur at 375 kHz. Increasing the slave loop length was an unmitigated success in the master loop.

Fig. 4(b) shows the phase noise data from the slave loop. Increasing slave loop length suppressed the first and second spurs by 28 and 8 dB respectively. In the long-slave-loop OEO, the spur levels rise as their offset frequencies approach that of the free-running slave spur. At 354 kHz, the long-slave-loop spur level is 17 dB higher than that of the short slave loop. However, the maximum spur level in the long slave loop (-113 dBc/Hz at 354 kHz) is 8 dB lower than the maximum spur level in the short slave loop (-105 dBc/Hz at 50 kHz). Furthermore, the phase noise at offset frequencies greater than 10 kHz is also reduced by increasing the slave loop length.

B. Coupling Strength

In order to better quantify our results, we utilize the following discrete performance parameters: the phase noise at 1 kHz; the phase noise at 10 kHz; and peak power of the first spur. The noise at 1 kHz and 10 kHz was estimated by taking the median noise levels in 100 Hz frequency-ranges around each frequency. The peak power at the first spur, refers to the first spur of the master. The spurious-mode power is measured between 40 and 60 kHz even in the case of the free-running slave. For each value of the coupling coefficient C, we measured the phase noise spectra in both the master and slave loops of the DIL-OEO. By recording the manner in which each parameter varied with the coupling coefficient, we were able to extract information that allowed us to optimize the DIL-OEO. In the following subsections, we outline the results of our systematic study.

1) Noise at 1 kHz: Fig. 5 shows the phase noise at 1 kHz versus the coupling coefficient for both free-running and injection locked master and slave loops. The free-running master and slave are single-loop OEOs. Increasing coupling from -20 dB to 0 dB, reduces the slave loop noise by 3 dB while leaving the master loop noise unchanged. Over the set of coupling coefficients used, the best noise performance at 1 kHz was obtained using 0 dB coupling. Using either 0 dB or -6 dB coupling ensures that the phase noise at 1 kHz of both master and slave loops are within 3 dB of the noise of the free-running master.

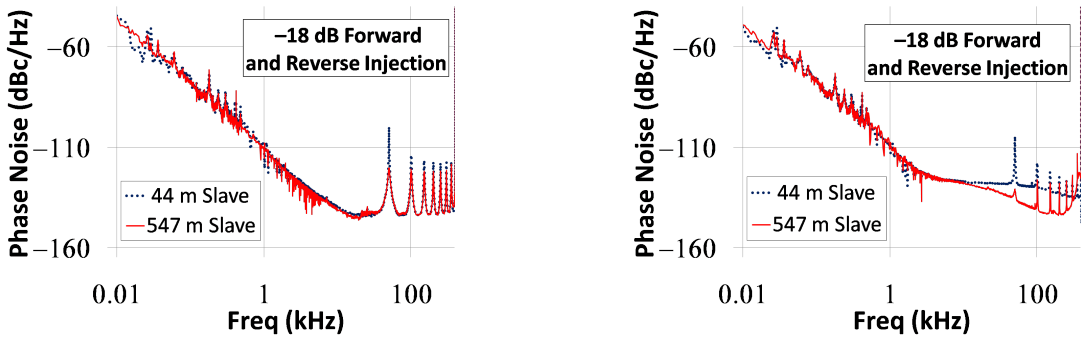

(a) Measured from the master loop.

(b) Measured from the slave loop.

Fig. 4. A comparison of the phase noise and spurious mode powers for two slave loop lengths.

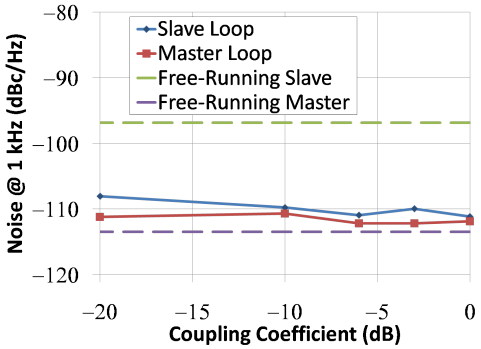

Fig. 5. Phase noise at 1 kHz versus the coupling coefficient. The data was collected from the injection-locked master and slave loops. Phase noise at 1 kHz for the free-running and master and slave are included for comparison.

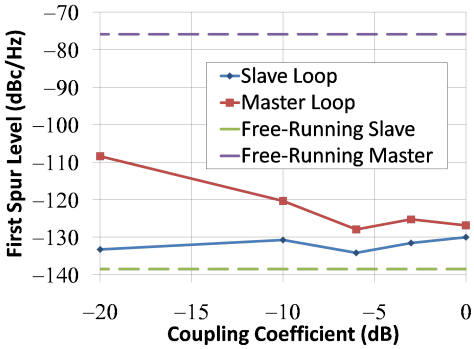

Fig. 7. Spur level versus the coupling coefficient. The data was collected from the injection-locked master and slave loops. Spur levels for the free-running and master and slave are included for comparison.

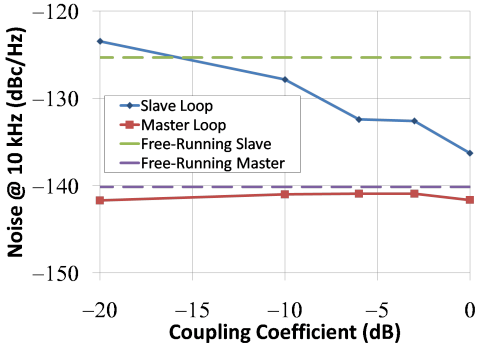

Fig. 6. Phase noise at 10 kHz versus the coupling coefficient. The data was collected from the injection-locked master and slave loops. Phase noise at 10 kHz for the free-running and master and slave are included for comparison.

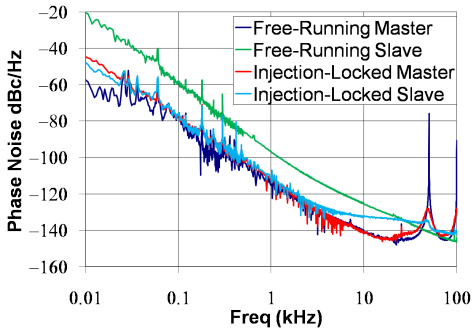

Fig. 8. Phase noise data from DIL-OEO with −6 dB coupling between master and slave loops. The phase noise was measured from both master and slave loops. Phase noise data from the free-running master and slave are included for comparison.

2) Noise at 10 kHz: Fig. 6 shows the effect of varying the coupling strength on the noise at 10 kHz. Again the effect of coupling in the slave loop is greater than in the master loop. Increasing coupling from −20 dB to 0 dB reduces the slave loop noise by 13 dB but has no effect on the master loop. Increased coupling has a much greater effect on the slave loop phase noise than on the phase noise of the master loop.

3) Peak Power at the First Spur: Fig. 7 shows the spur level versus the coupling strength in both the master and slave. A coupling of−6 dB generates the lowest spurs in both loops. The lowest master loop spur level is −128 dBc/Hz, which is 50 dB lower than that of the free-running master. The lowest spur level in the slave is −134 dBc/Hz, which is within 4 dB of the noise level of the free-running slave at the same offset frequency.

C. The Optimized DIL-OEO

Fig. 8 shows the phase noise data of the optimized DIL-OEO. A coupling ratio of -6 dB provides the best combination of low phase noise and low spur levels in both the master and slave loops. The slave loop signal in particular, benefits from increased coupling. We managed to reduce the spur level to within 4 dB of the noise level of the free-running slave while reducing the phase noise at 1 and 10 kHz by 13 and 7 dB respectively. The noise penalty relative to the free-running master is 8 dB at 10 kHz and less than 3 dB at 1 kHz, whereas the spur reduction is over 60 dB. Our experimental results are consistent with the predictions of both our previously reported analytical and numerical models [5], [6].

IV. Conclusion

We investigated the effects of slave loop length and coupling strength on the steady-state signal of the DIL-OEO. We found that increasing coupling strength reduced spurious modes in the master while also reducing phase noise in the slave. Increasing slave loop length also improved spurious mode suppression in the master.

We have experimentally constructed a DIL-OEO with the low phase noise of a long loop OEO and the spurious mode levels of a short loop OEO. Our results demonstrate that the dual injection-locked OEO is capable of combining the high-Q of a long cavity OEO with the quasi-singlemode behavior of a short loop OEO. Having overcome the Q versus mode-spacing dilemma, we have demonstrated that the DIL-OEO is a practical and inexpensive source of low phase noise microwave signals in RF and RF-photonic applications.

Acknowledgment

The authors would like to thank DARPA for funding this research.

References

[1] X. S. Yao and L. Maleki, "Optoelectronic microwave oscillator," *J. Opt. SOc. Am. B*, vol. 13, no. 8, pp. 1725–1735, 1996.

[2] ——, "Optoelectronic oscillator for photonic systems," *IEEE J. Quantum Electron.*, vol. 32, no. 7, pp. 1141–1149, Jul. 1996.

[3] D. A. Howe and A. Hati, "Low-noise X-band oscillator and amplifier technologies: Comparison and status," in *Proceedings of the Joint IEEE International Frequency Control Symposium and Precise Time and Time Interval (PTTI) Systems and Applications Meeting*, Vancouver, Canada, Aug. 2005, pp. 481–487.

[4] O. Okusaga, W. Zhou, E. C. Levy, M. Horowitz, G. M. Carter, and C. R. Menyuk, "Experimental and simulation study of dual injection-locked OEOs," in *Proceedings of Joint Meeting of the European Frequency and Time Forum and the IEEE International Frequency Control Symposium*, Besancon, France, Apr. 2009, pp. 875–879.

[5] C. R. Menyuk, E. C. Levy, O. Okusaga, M. Horowitz, G. M. Carter, and W. Zhou, "An analytical model of the dual-injection-locked opto-electronic oscillator (DIL-OEO)," in *Proceedings of Joint Meeting of the European Frequency and Time Forum and the IEEE International Frequency Control Symposium*, Besancon, France, Apr. 2009, pp. 870–874.

[6] E. C. Levy, M. Horowitz, and C. R. Menyuk, "Modeling optoelectronic oscillators," *J. Opt. SOc. Am. B*, vol. 26, no. 1, pp. 148–159, 2009.